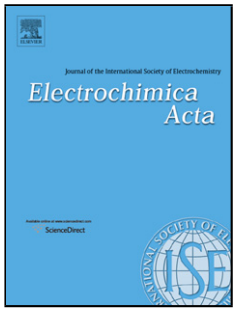

Title: Electrochromic and electrochemical capacitive properties of tungsten oxide and its polyaniline nanocomposite films obtained by chemical bath deposition method

Author: Chinwe A. Nwanya Charl J. Jafta Paul M. Ejikeme Paulinus E. Ugwuoke M.V. Reddy Rose U. Osuji Kenneth I. Ozoemena Fabian I. Ezema<ce:footnote id="fn0005"><ce:note-para id="npar0005">ISE student member.</ce:note-para></ce:footnote><ce:footnote id="fn0010"><ce:note-para id="npar0010">ISE member.</ce:note-para></ce:footnote>

PII: S0013-4686(13)01881-1
DOI: http://dx.doi.org/doi:10.1016/j.electacta.2013.10.002
Reference: EA 21336

To appear in: *Electrochimica Acta*

Received date: 25-7-2013
Revised date: 24-9-2013
Accepted date: 1-10-2013

Please cite this article as: C.A. Nwanya, C.J. Jafta, P.M. Ejikeme, P.E. Ugwuoke, M.V. Reddy, R.U. Osuji, K.I. Ozoemena, F.I. Ezema, Electrochromic and electrochemical capacitive properties of tungsten oxide and its polyaniline nanocomposite films obtained by chemical bath deposition method, *Electrochimica Acta* (2013), http://dx.doi.org/10.1016/j.electacta.2013.10.002

Electrochromic and electrochemical capacitive properties of tungsten oxide and its polyaniline nanocomposite films obtained by chemical bath deposition method

Chinwe A. Nwanya[a,1], Charl J. Jafta[b,1], Paul M. Ejikeme[c,1], Paulinus E. Ugwuoke[a], M.V. Reddy[d], Rose U. Osuji[e], Kenneth I. Ozoemena[b,2] and Fabian I. Ezema[e,*2]

[a]*National Centre for Energy Research and Development, University of Nigeria Nsukka*

[b]*Energy Materials, Materials Science & Manufacturing, Council for Scientific & Industrial Research (CSIR), Pretoria 0001, South Africa*

[c]*Department of Pure and Industrial Chemistry, University of Nigeria, Nsukka*

[d]*Department of Physics, Solid State Ionics & Advanced Batteries Lab, National University of Singapore, Singapore 117542*

[e]*Department of Physics and Astronomy, University of Nigeria, Nsukka*

Abstract

* Author to whom corresponding should be addressed (FI Ezema): Tel.: +234-8036239214
E-mail address: fiezema@yahoo.com

[1] ISE student member

[2] ISE member

Polyanine and its nanocomposite WO_3/PANI films were deposited on Fluorine doped tin oxide (FTO) glass slides by simple Chemical Bath Deposition Method. The morphology and crystalline structure of the composite film was studied using Atomic force (AFM) and Scanning Electron Microscopy, while the electrochemical capacitive properties were determined using Cyclic Voltammetry (CV), chronopotentiometry (CP) and electrochemical impedance spectroscopy (EIS). The WO_3 / PANI nano-composite exhibited multiple colors (electrochromism) during the CV scans, from brownish green to transparent to light green then back to brownish green. Surprisingly, the integration of the PANI with the WO_3 led to synergistic performance of nanohybrid wherein a true electrochemical double layer capacitor was obtained. Also, interestingly and unlike literature reports, the CBD method led to excellent capacitance retention (> 98%) of the PANI even at 1000 continuous cycles. This work demonstrates that simple CBD can be used to get WO_3 / PANI films that give good electrochromism and pseudo-capacitance comparable to the ones obtained by other methods. Hence the obtained nanocomposite film of WO_3 / PANI can be a promising material for electrochromic and energy storage applications.

Key words: Chemical bath deposition; PANI film; WO_3/PANI film; Electrochromism; Electrochemical capacitors.

1.0 Introduction

Tungsten oxide (WO_3) is an attractive transition metal oxide that has been widely studied due to its multifunctional properties that leads to a wide range of applications. It has shown good electrochromic, optochromic and gasochromic properties [1-3]. Tungsten oxide's band gap is within the solar spectrum range making it one of the solar energy materials for photo catalytic, photoconductivity and photovoltaic applications [4, 5]. The electrochromic (EC) effect, i.e. a reversible color change induced by an electric field of WO_3 was first reported by Deb in 1969 [3] and is considered the best material for EC applications due to its high coloration efficiency [6, 7].

Various models have been proposed to explain the EC mechanism in WO_3. One of such is that by Schirmer et al [8], in which they proposed that the optical absorption of the films is caused by the small polaron (SP), or transitions between two non-equivalent sites of tungsten (W^{+5} and W^{+6}):

$$h\nu + W^{+5}(A) + W^{+6}(B) \rightarrow W^{+5}(B) + W^{+6}(A) \qquad 1$$

According to this model, inserted electrons are localized in W^{+5} sites and polarize their surrounding lattice to form small polarons. It is widely believed that WO_3 thin films undergo a chemically reversible electron and cation intercalation reaction to form tungsten bronzes (M_xWO_3) during coloration and an electron and cation deintercalation reaction during bleaching [7, 9] according to the following equation:

$$WO_3 + xM^+ + xe^- \leftrightarrow M_xWO_3 \qquad 2$$

where $M^+ = H^+, Li^+, etc$

Conducting polymeric materials like polypyrrole (PPy), Polyaniline (PANI) and polythiopheres etc. have been considered as EC materials but among these, PANI has emerged as the most promising active materials for electrochromic devices due to its high capacitive characteristics, relative ease in preparation, good environmental stability and tuneable conductivity [10]. PANI has been shown to give four distinct colors corresponding to four redox states which are: yellow (leucoemeraldine base), green (emeraldine salt), blue (emeraldine base) and purple (pernigraniline base) [11]. One drawback of polyaniline film is that it shows low conductivity where it can affect its electrochromic behavior [12]. To improve the performance of PANI, some conductive fillers are introduced in the PANI structure forming nanocomposites. The aim is to obtain materials with synergetic or complementary properties to PANI. Some of those improvements were shown by Wei et al [13], using nanocomposite of PANI and graphite oxide. Others include the works done by Gupta and Miura [10], Shahazmi et al, [12] using PANI/carbon nanotube composite, PANI/ZnO nanocomposite [14, 15], PANI/WO_3 nanocomposte [16-22] etc.

WO_3 along with some other transition metal oxides and some conducting polymers have also been considered as good materials for psuedocapacitors. Among these, the most intensively investigated is Ruthenium oxide (RuO_2) which has been shown to give appreciable specific capacitance of up to 1500Fg^{-1} over a wide potential range of 1.4V [23-25] but its commercial application is limited due to high cost and high toxicity. To reduce the cost of RuO_2 some low cost metal oxides such as NiO, CoOx and MnO_x etc. have been investigated as electrode materials for electrochemical capacitors [26, 27]. Nano-composites of these metal oxides with high surface area carbon materials have been shown to enhance the capacitance as

reported by Zheng et al [28]. Although tungsten oxides especially in its crystalline state shows little capacitance, the pseudocapacitive properties of amorphous tungsten oxide synthesized by microwave irradiation investigated over the potential range of 0–0.5V vs SCE displayed a volumetric capacitance of 231Fcm^{-3} [29]. The high specific capacitance was ascribed to the participation of proton provided by the tungsten oxide.

Conducting polymers like PANI, PPy and polythiopheres are also good materials for electrochemical capacitors due to their excellent capacity for energy storage, slow charge discharge, easy synthesis, high energy and power density and good chemical stability. The shortcoming of these polymers is the degradation that occurs due to its swelling and shrinking during cycling. This occurs because the insertion and removal of ions causes a volume change in the polymer. This problem is overcome by the use of composite structures as indicated earlier. Hybrid organic/inorganic materials in general represent the natural interface between two worlds of material science. The main challenge is managing to synthesize inorganic–organic hybrid combinations that keep or enhance the best properties of each of the components while eliminating or reducing their particular limitations. Tungsten oxide shows electroactivities over comparatively negative potential range and is a cathodic EC material which changes color from transparent or yellow to deep blue with large optical modulation when it is reduced by H^+ or Li^+ while PANI is an anodic coloration material [9, 30]. Nano-composite film of WO_3/ PANI tends to enhance the properties of the two materials singly while reducing their shortcomings.

Quantitative parameters of the electrochromic and psuedocapacitive properties of tungsten oxide and PANI strongly depend on its structural, morphological and compositional characteristics and, therefore on the deposition techniques and deposition parameters. WO_3

thin film is deposited by various techniques including physical vapor deposition (thermal evaporation and sputtering) [31-32], electrochemical methods [33] and chemical methods (sol-gel and hydrothermal approach) [5, 34-35]. PANI thin films is mainly prepared by the oxidation of aniline oligomer with ammonium peroxydisulfate in acidic aqueous medium [36-37] and by electrochemical deposition method [16-18, 38]. One major disadvantage of WO_3 is that it has a slow response time compared to other electrochromic materials like NiO etc. [6] while PANI gives a relatively low electrochemical stability [16]. This imposes a challenge to their applications.

In this paper we investigate the electrochromic and electrochemical capacitive properties of nancomposite film of WO_3/PANI obtained by a simple chemical bath deposition (CBD) method. The enhancement of electroactivity within the applied potential window without losing any electroactivity due to the presence of the component is advantageous for the utilization of such composites for electrochromic and super capacitive applications. To the extent of our knowledge, the electrochromic and electrochemical capacitive properties of this nanocomposite deposited by this method has not been investigated. Most of the work that investigated these properties for the nanocomposite deposited PANI on WO_3 electrochemically. However, the electrochromically deposited polyaniline exhibit substantial resistivity, which is attributed to the lack of conducting pathways at the nanoscale associated with random deposition morphology [12]. Also, CBD method offers greater advantage for easy scale-up for commercialization than electrochemical deposition. In this work, we clearly show that the CBD method provides much higher energy storage properties compared to the values reported for electrochemical deposition. The morphology and structure of the composite films were studied

using Atomic Force Microscopy (AFM) and Scanning Electron Microscopy (SEM). The optical properties were investigated using UV-VIS spectroscopy while the capacitive behaviors of the films for electrochromic and energy storage device applications were investigated using cyclic voltammetry, galvanostatic charge-discharge cycling and electrochemical impedance spectroscopy.

2.0 Experimental Details

2.1 Deposition of Tungsten oxide (WO_3)

WO_3 was deposited on fluorine doped tin oxide (FTO) coated glass substrates (resistance 17-30Ω) using simple chemical bath deposition method. The deposition conditions (temperature, concentrations, time of deposit and pH) were optimized and we arrived at hydrolyzing 0.07M sodium tungstate ($Na_2WO_4.2H_2O$) in distilled water. The deposition is pH dependent hence 0.6M HCl was added to the solution to get a pH of 5. The volume ratio of $Na_2WO_4\ 2H_2O$:HCl was 1:1. The FTO substrates which have been cleaned with detergent and water, rinsed with distilled water and sonicated in distilled water for 5mins were immersed into the solution and the bath temperature kept at 40^{o}C. The deposition time was varied but the sample we used for this analysis was deposited after 7hr. The films were then removed and rinsed with distilled water. It was found that at higher concentration of the $Na_2WO_4\ 2H_2O$, the solution precipitates and gives no deposit while at room temperature the reaction is incomplete resulting also to lack of deposit. At higher temperature the solution precipitates quickly. The films were annealed at 400^{o}C during which the color changed from white to milky color.

2.2 Tungsten oxide / polyaniline nanocomposite (WO_3 / PANI)

PANI films were deposited by oxidation of aniline in an acidic aqueous medium using ammonium peroxydisulfate as the oxidant. 0.25 M ammonia persulfate was dissolved in 60ml of 1 M HCl to which 2 mL of aniline is added. The deposition was at room temperature and time of deposit was one 1hr after which the film was rinsed with distilled water and air dried. To get thicker films the above process was repeated for up to five times (1-5 deposit times). It was noticed that the polymerization reaction is completed by 1hr after which the solution precipitates and no more deposit occur on the substrates even if it is left in the solution for longer period of time. To get the WO_3 / PANI nanocomposite, the FTO with already deposited WO_3 thin films were immersed into the solution prepared for PANI and the bath temperature kept at room temperature. The films were removed and rinsed with distilled water after one hour.

2.3 Characterization techniques

The surface morphology of the films was studied using Atomic Force Microscopy (AFM) and scanning electron microscopy (SEM). The AFM measurements were carried out with a commercial Agilent 5500 AFM (Agilent technologies, USA) in the acoustic mode (also known as tapping mode) at a scanning rate of 1 Hz. The Si cantilevers used had a nominal resonant frequency of ~ 230 kHz and a nominal force constant of ~ 50 N/m. The UV-VIS-NIR spectrophotometer was used to get the optical properties of the film in the wavelength range of 300 – 900 nm. The electrochemical properties were investigated by Cyclic Voltammetry (CV) at different scan rates in 0.5 M H_2SO_4 aqueous solution. The capacitative performances were

investigated by galvanostatic charge–discharge and electrochemical impedance spectroscopy (EIS). The EIS was done between 100 kHz and 10 MHz using an Autolab potentiostat PGSTAT 302N (Eco Chemie, Utrecht, Netherlands) making use of the general purpose data processing software (GPES and FRA version 4.9).

3.0 Results and Discussions

3.1 Growth kinetics and the mechanism of the films formation.

The WO_3 thin films were prepared by simple CBD method using sodium tungstate ($Na_2WO_4.2H_2O$) and HCl as the precursors. The growth mechanism of the WO_3 takes place as follows: Sodium tungstate is a white crystalline powder that is soluble in water and dissociate according to equation [7,9]

$$\mathrm{Na_2}WO_4 2H_2O + H_2O \rightarrow WO_{4(aq)}^{2-} + 2Na_{(aq)}^{+} + 2H_3O^{+} \quad 3$$

On addition of the HCl, tungstic acid is formed and the following reaction in equation 3 is the most probable. The tungstic acid adsorbed to the FTO substrate in the bath which on heating gives the tungsten trioxide.

$$2WO_{4(aq)}^{2-} + Na_{(aq)}^{+} + H_3O^{+} + HCl \rightarrow WO_3..H_2WO_4 + NaCl + H_2O \quad 4$$

$$WO_3..H_2WO_4 + heat \rightarrow 2WO_{3(s)} + H_2O \quad 5$$

Aniline oligomers are first produced during the oxidation of aniline in an acidic aqueous medium. These Aniline oligomers are more hydrophobic than the original anilinium cations hence they have a tendency to separate from the aqueous medium by adsorbing themselves at available surfaces in contact with aqueous reaction mixture [37]. Practically any substrate

present in the reaction mixture used for the oxidation of aniline becomes coated with a thin PANI film. The first adsorbed oligomers initiate the growth of PANI chain by anchoring on the FTO and producing the nucleus of the future film. Then the new oligomers adsorb close to the nucleus, and stimulate the growth of new PANI chains. According to Sapurina et al, [39] the PANI chain that forms a film proliferates along the surface orients preferentially perpendicularly to the substrate. The WO_3 particles are then distributed in the PANI chain to form the composite film.

Morphology Analysis

The SEM of WO_3 and WO_3/PANI are shown in Figure 1. The WO_3 film shows spherical grains spread irregularly all over the surface while the WO_3 / PANI shows micro aggregates with a larger active surface area than that of pure WO_3. This micro-porous structure with high specific area may provide more opportunity for the reactive centers on the film to contact with electrolyte and so aid the charge transfer in the bulk of the film. AFM surface morphologies of the films are shown in Figure 2. The composite film showed morphology slightly different from that of the WO_3 indicating the possible presence of PANI distributed in the network of WO_3.

3.2 Optical properties of the films

The absorbance spectrum of the thin films is shown in Figure 3. The bandgap E_g of the thin films was estimated from the absorbance spectra using equation 6 [40]:

$$E_g = \frac{1240}{\lambda_{edge}} \qquad 6$$

where E_g is the optical bandgap in eV and λ_{edge} is the absorption edge in nm. The λ_{edge} for the films were around 450, 503 and 350 nm while the estimated E_g values are 2.7, 2.4, 3.5eV for the PANI, WO_3/PANI and WO_3 films respectively. The fully reduced and insulating form (leucoemeraldine base, LB) of PANI exhibits larger bandgap (higher than 3eV) while the fully oxidized and semiconducting form (pernigraniline base, PNB) possess a lower bandgap (lower than 2 eV) [41]. The band gap of the nanocomposite is close to the reported value of 2.29 eV for PANI doped with MWNT [42]. The reduced band gap for the composite also makes this material desirable for other applications such as photoelectrochemical cells for solar energy conversion or water splitting to generate water.

3.3 Cyclic Voltammetry of the films

Figure 4 compares the cyclic voltammetric evolutions of the films immobilized on FTO glass recorded in 0.5 M H_2SO_4 solution in a potential window of -0.6 to +0.8 V. The PANI film showed two redox couples, (I)/II) and (III)/(IV) arising from the transitions between leucoemeraldine (LS) / emeraldine salt (ES) and emeraldine salt (ES) / pernigraniline salt (PS) of PANI, respectively. Peak potential separation has been used to determine the reversibility of an electrochemical redox reaction. The WO_3 film showed weak redox couple (V) around –0.1 V, which is related to the intercalation / de-intercalation of H^+ [36]. The anodic potential scan causes the de-intercalation of H^+ ions giving rise to the bleaching of the film due to the oxidation of W^{+5} to W^{+6} while the cathodic scan causes simultaneous intercalation of e^-s and H^+ ions into the films giving rise to the reduction of W^{6+} to lower valence W^{+5} state hence the films get colored. The development of two peaks could be attributed to two types of H^+

injection site: reversibly active and shallow trap site [36]. It should be seen from the comparative CVs that the peak-to-peak separations (ΔE_p) between the anode and cathodic waves for the PANI film are much larger than for the nanocomposite WO_3/PANI film, indicating that the composite film exhibits enhanced reversible redox reactions than the PANI alone. Each CV curve consists of a pair of redox peaks, which indicates that the capacitance characteristics are mainly governed by Faradaic reactions (i.e., pseudocapacitive properties). The CV at various scan rates for the composite film (Figure 4b) shows that the peaks gets more pronounced with increased scan rate.

The nanocomposite WO_3 / PANI film showed multiple peaks corresponding to the redox pairs of WO_3 and PANI. A reduction of the peak currents of about 0.2mA could be observed for the composite film with respect to pure PANI film. This could be due to the formation of a donor (PANI)-acceptor (WO_3) system [43]. The composite exhibited electrochromic behavior (multiple coloration) during the scanning process, from brownish green to transparent to light green then back to brownish green (Figure 5).

The capacitance (C) of the films was calculated using the following relation [44]:

$$C = \frac{I_{max}}{dv/dt} \qquad 7$$

where I_{max} is the maximum current in ampere and dV/dt is the voltage scanning rate. The specific capacitance (F/cm^2) was calculated using the relation:

$$C_s = \frac{C}{A} \qquad 8$$

where A is the area of the active material dipped in the electrolyte. The capacitance of the composite film obtained is 10 mF/cm^2 while that of WO_3 and PANI are 4 and 17 mF/cm^2 respectively at a scan rate of 50 mV/s. The values obtained for the composite film is comparable to 25 mF/cm^2 obtained at a much low scan rate of 5 mV/s by Wei et al. [16].

3.4 Galvanostatic charge–discharge analysis

The galvanostatic charge–discharge (GCD) measurements give more reliable data than CV measurements for capacitance [45], thus GCD test were carried out on the films in a three-electrode system with 0.5M H_2SO_4 at 0.02 mA cm^{-2} (Figure 6a). The potential responses of the composite film during charge and discharge are more symmetrical than that of the WO_3 and the absolute working potential window can be extended to 1.0V. The shape of the discharge curves does not show the characteristic profile of a pure double layer capacitor, but mainly pseudocapacitance. The slope of the charge/discharge curves indicates the potential dependent nature of the Faradaic reaction [46].

The areal capacitance (C_A) can be calculated using the following equation [13,47]:

$$C_A = \frac{i \times \Delta t}{\Delta V \times A} \qquad 9$$

where i is the applied current in A, ΔV the voltage range in Volt, Δt the discharge time in seconds and A the active area in cm^2.

The dependence of the specific capacitance on current density are shown in Figure 6b. The specific capacitance of the composite film (WO_3 / PANI) derived from the discharge in the

charge-discharge curve is 4.1 mF/cm^2 at a current density of 0.02 mA/cm^2 and 2.4 mF/cm^2 at a higher current density of 0.16 mA/cm^2. WO_3 is seen to display very quick discharge times at higher current densities with a potential overshoot to approximately 1.1 V due to its high resistance. Its specific capacitance at current densities of 0.02 mA/cm^2 and 0.16 mA/cm^2 are 2.8 mF/cm^2 and 0.3 mF/cm^2, respectively. The areal capacitance of the WO_3 is improved by the incorporation of PANI due to the distribution of WO_3 particles in the network of PANI.

Table 1: Maximum performance parameters of the electrodes

Electrode	C_A (F cm^{-2})
WO_3	2.8
WO_3/PANI	4.1
PANI	9.2

From table 1 it is evident that the areal capacitance of the PANI is superior, with the composite WO_3/PANI beating the WO_3.

Next, we studied the long-term cyclability of the films by performing repetitive repetitive charge-discharge cycling for 1000 cycles lasting about 2 days (Figure 7). It is clearly evident from Figure 7 that at the 800th cycle, the WO_3 film retained only 21% of its original capacitance, while the WO_3/PANI and PANI retained approximately 38% and 98% of their starting capacitance values at the 1000th cycle, respectively. Again, this is an interesting result as it contradicts the works of Wei et al. [13,16] that reported that PANI film formed by electropolymerisation lost most of its capacitance after the 350th cycle. Our result implies that the CBD method represents a more viable strategy than electro-polymerisation for the preparation of the PANI films for electrochemical capacitors. The reason for the improved

performance of the CBD is not clear at the moment, but may be related to the possible improvement of the physico-chemical homogeneity of the polymer (PANI) that allows for enhanced mobility of the counter ions. Conducting electro-polymers are usually characterised to the so-called negative 'redox-switching hysteresis [45].

3.5 Electrochemical Impedance Spectroscopy

Electrochemical impedance spectroscopy (EIS) was employed to provide further some insights into the electrochemical acapacitive behavior of the three films. Figure 8 displays the Nyquist plots of the films performed in 0.5M H_2SO_4 at 0.1 V vs Ag/AgCl (sat'd KCl) before (Fig.8a) and after (Fig. 8b) the 1000^{th} cycle. To our surprise, the WO_3/PANI did not show any resistive component (i.e., the real impedance Z' is zero) even after the 1000^{th} cycle, which is characteristic of a 'pure capacitive' or electric double layer capacitor (EDLC) behaviour. On the other hand, the PANI and WO3 films showed resistive properties. Also, from the Bode plots (Figure 9), the phase angles of the PANI and WO_3/PANI films are -67.3^{o} and -89.0^{o}, respectively. Pure capacitive behaviour should give a phase angle of -90^{o}, thus our Bode results again confirm the pure EDLC behavior of the composite compared to the PANI alone. The ''knee'' or ''onset'' frequency (f_o) for the WO3/PANI film 4.9 Hz while that of the PANi alone is 0.82 Hz, suggesting that most of the stored energy of the WO3/PANI is still accessible at higher frequencies compared to the PANI film.

4.0 Conclusion

Simple Chemical Bath deposition (CBD) method has been used to prepare polyanilline and its nanocomposite film of WO_3/PANI on fluorine doped tin oxide (FTO) glass slides. The composite

film exhibited electrochromic behaviour during the cyclic voltammetry. The key findings in this work that we need to emphasize are (i) the PANI films is able to maintain its energy storage capability even at 1000 cycles, and (ii) the integration of the PANI with WO_3 led to the formation of a true electrochemical capacitor. This work demonstrates that simple CBD can be used to get WO_3/PANI film that gives good electrochromic and pseudo capacitance comparable to the ones obtained by other methods. Hence the obtained nanocomposite film of WO_3/PANI can be a promising material for electrochromic and energy storage applications.

Acknowledgments

The authors (from the UNN) thank the US Army Research Laboratory–Broad Agency Announcement (BAA) for the financial support given to this research (under Contract number W911NF-12-1-0588). We gratefully acknowledged the support from the CSIR and DST/NRF Nanotechnology Flagship Programme (South Africa) during the recent research visit to the CSIR.

References

1. E. Rossinyol, A. Prim, E. Pellicer, J. Arbiol, F. Hernández-Ramírez, F. Peiró, A. Cornet, J.□R. Morante, L.□A. Solovyov, B. Tian, T. Bo, and D. Zhao, Synthesis and characterization of chromium-doped mesoporous tungsten oxide for gas-sensing applications, Advanced Functional Materials, 17, (2007), 1801–1806.
2. T. He and J. Yao, Photochromic materials based on tungsten oxide, Journal of Materials Chemistry, 17, (2007), 4547–4557.
3. S. Deb, Novel Electro-photographic System, Applied Optoelectronics, 3, (1969), 192-193.

4. E. Stathatos, P. Lianos, U. Lavrencic-Stangar and B. Orel, A high-performance solid-state dye-sensitized photoelectrochemical cell employing a nanocomposite gel electrolyte made by the sol-gel route, Advanced Materials, 14, (2002),354–357.
5. Z. Jiao, J. Wang, L. Ke, X. W. Sun, D H. V. emir, Morphology-Tailored Synthesis of Tungsten Trioxide (Hydrate) Thin Films and Their Photocatalytic Properties, ACS Appl. Mater. Interfaces 3, (2011), 229–236
6. A.I. Inamdar, A.C. Sonavane, S.M. Pawar, Y. Kim, J.H. Kim, P.S. Patil, W. Jung, H. Im, D-Y. Kim and H. Kim, Electrochromic and Electrochemical Properties of Amorphous Porous Nickel Hydroxide thin films, Applied Surface Science, 257, (2011), 9606-9611.
7. R.R. Kharade, S.R. Mane, R.M. Mane, P.S. Patil and P.N. Bhosale, Synthesis and characterization of chemically grown electrochromic tungsten oxide, Journal of Sol-Gel Science Technology, 56, (2010), 177-183.
8. O.F. Schirmer, J. Phys (Paris), Colloque 6: (1980), 479.
9. M.A. Aegerter, Sol-Gel Chromogenic Materials and Devices, Structure and Bonding, 85, (1996), 149-194.
10. V. Gupta and N. Miura, Polyaniline/single-wall carbon nanotube (PANI/SWCNT) composites for high performance supercapacitors, Electrochimica Acta, 52, (2006), 1721-1726.
11. L. Zhao, L. Zhao, Y. Xu, T. Qiu, L. Zhi and G. Shi, Polyaniline electrochromic devices with transparent graphene electrodes, Electrochimica Acta, 55, (2009), 491-497.
12. M. S. M. Zambri, N. M. Mohamed and C. F. Kait, Preparation of Electrochromic Material Using Carbon Nanotubes (CNTs), Journal of Applied Sciences, 11, (2011), 1321-1325.

13. H. Wei, J. Zhu, S. Wu, S. Wei, Z. Guo, Electrochromic Polyaniline/Graphite Oxide Nanocomposites with Endured Electrochemical Energy Storage, Polymer, 54, (2013), 1820-1831

14. S.B. Kondawar, S.A. Acharya, S.R. Dhakate, Microwave assisted hydrothermally synthesized nanostructure zinc oxide reinforced polyaniline nanocomposites, Advanced Materials Letters, 2, (2011), 362-367.

15. S. P. Ansari and F. Mohammad, Studies on Nanocomposites of Polyaniline and Zinc Oxide Nanoparticles with Supporting Matrix of Polycarbonate, ISRN Materials Science Volume 2012, Article ID 129869, 2012, 7 pages doi:10.5402/2012/129869

16. H. Wei, X. Yan, S. Wu, Z. Luo, S. Wei and Z. Guo, Electropolymerized Polyaniline stabilized Tungsten oxide Nanocomposite film: Electrochromic Behavior and Electrochemical Energy Storage, The Journal of Physical Chemistry C., 116, (2012), 25052-25064.

17. S.S. Kalagi, S.S. Mali, D.S. Dalavi, A.I. Inamdar, H. Im and P.S. Patil, Limitations of dual and complementary inorganic–organic electrochromic device for smart window application and its colorimetric analysis, Synthetic Metals, 161, (2011), 1105–1112

18. B-X. Zou, Y. Liang, X-X. Liu, D. Diamond, and K-T. Lau, Electrodeposition and pseudocapacitive properties of tungsten oxide/polyaniline composite, Journal of Power Sources 196, (2011), 4842–4848

19. Ben-Xue Zou, Ying Liang, Xiao-Xia Liu, Dermot Diamond, King-Tong Lau, Electrodeposition and pseudocapacitive properties of tungsten oxide/polyaniline composite, Journal of Power Sources 196 (2011) 4842–4848

20. Electrodeposited Polyaniline in a Nanoporous WO3 Matrix: An Organic/Inorganic Hybrid Exhibiting Both p-and n-Type Photoelectrochemical Activity, Csaba Janaky, Norma R. deTacconi, Wilaiwan Chanmanee, and KrishnanRajeshwar.Phys. Chem. C (2012),116, 4234−4242

21. Jun Zhang, Jiang-ping Tu, Dong Zhang, Yan-qiang Qiao, Xin-hui Xia, Xiu-li Wang and Chang-dong Gu, Multicolor electrochromic polyaniline–WO3 hybrid thin films: One-pot molecular assembling synthesis, J. Mater. Chem., (2011), 21, 17316–17324

22. Narsimha Parvatikar, Shilpa Jain, Syed Khasim, M.Revansiddappa, S.V. Bhoraskar, M.V.N. Ambika Prasad Electrical and humidity sensing properties of polyaniline/WO3 composites Sensors and Actuators B114 (2006) 599–603

23. J.-K. Lee, H.M. Pathan, and K.-D. Jung, Electrochemical capacitance of nanocomposite films formed by loading carbon nanotubes with ruthenium oxide, Journal of Power Sources 159, (2006), 1527-1531.

24. S.C. Pang, M. A. Anderson, and T.W. Chapman, Novel Electrode Materials for Thin-Film Ultracapacitors: Comparison of Electrochemical Properties of Sol-Gel-Derived and Electrodeposited Manganese Dioxide, Journal of Electrochemical Soc. 147, (2000), 444-450.

25. C.C. Hu, Y.H. Huang and K. H. Chang, Annealing effects on the physicochemical characteristics of hydrous ruthenium and ruthenium–iridium oxides for electrochemical supercapacitors, Journal of Power Sources, 108, (2002), 117-127.

26. S.G. Kandalkar, J.L. Gunjakar and C.D. Lokhande, Preparation of cobalt oxide thin films and its use in supercapacitor application, Applied Surface Science, 254,(2008), 5540-5544.

27. J-K. Chang, C-H. Huang, and W-T. Tsai, Manganese films electrodeposited at different potentials and temperatures in ionic liquid and their application as electrode materials for supercapacitors, Electrochimica Acta, 53, (2008), 4447- 4453.

28. J.P. Zheng, P.J. Cygan, and T.R. Jow, Hydrous Ruthenium Oxide as an Electrode Material for Electrochemical Capacitors, Journal of Electrochemical Soc. 142, (1995), 2699-2703.

29. C.-C. Huang, W. Xing and S-P. Zhuo, Capacitive performances of amorphous tungsten oxide prepared by microwave irradiation, Scripta Materialia, 61, (2009), 985-987.

30. B-X Zou, X-X. Liu and D. Diamond, Electrochemical synthesis of WO_3/PANI composite for electrocatalytic reduction of iodate, Electrochimica Acta 55, (2010), 3915-3920.

31. M.U. Qadria, M.C. Pujol, J. Ferré-Borrull, E. Llobet, M. Aguiló and F. Díaz, WO_3 thin films for optical gas sensing, Procedia Engineering, 25, (2011), 260 – 263.

32. R. Azimirad, O. Akhavan and A. Z. Moshfegh, The effect of heat treatment on physical properties of nanograined (WO_3)- (Fe_2O_3)x thin films, Vacuum, 85, (2011), 810-819.

33. M. Metikosˇ-Hukovic´, and Z. Grubacˇ, The growth kinetics of thin anodic WO_3 films investigated by electrochemical impedance spectroscopy, Journal of Electroanalytical Chemistry 556, (2003),167-178.

34. H. Choi, B.S. Kim, M.J. Ko, D-K. Lee, H. Kim, S.H. Kim, K. Kim, Solution processed WO_3 layer for the replacement of PEDOT: PSS layer in organic photovoltaic cells Organic Electronics 13, (2012), 959–968.

35. W. Cheng, E. Baudrin, B. Dunn and J.J. Zink, Synthesis and Electrochromic properties of Mesoporous tungsten oxide, Journal of Materials chemistry, 11, (2001), 92-97.

36. I. Sapurina, N.E. Kazantseva, N.G. Ryvkina, J. Prokeš, P. Sáha and J. Stejskal, Electromagnetic radiation shielding by composites of conducting polymers and wood, Journal of Applied Polymer Science 95, (2005), 807-814.

37. J. Stejskal and I. Sapurina, Polyaniline: Thin Films And Colloidal Dispersions, Pure Applied Chemistry, 77, (2005), 815–826, DOI: 10.1351/pac200577050815

38. D.S. Dhawale, R.R. Salunkhe, V.S. Jamadade, T.P. Gujar, C.D. Lokhande, An approach towards the growth of Polyaniline nanograins by electrochemical route, Applied Surface Science, 255, (2009), 8213-8216.

39. I. Sapurina, A. Y. Osadchev, B. Z. Volchek, M. Trchová, A. Riede, J. Stejskal, In-situ polymerized polyaniline films: 5. Brush-like chain ordering, Synthetic Metals, 129, (2002), 29-37.

40. C. Bora and S. K. Dolui, Fabrication of polypyrrole/graphene oxide nanocomposites by liquid/liquid interfacial polymerization and evaluation of their optical, electrical and electrochemical properties, Polymer, 53, (2012), 923-932.

41. O. Kwon and M. L. McKee, Calculations of Band Gaps in Polyaniline from Theoretical Studies of Oligomers, J. Phys. Chem. B, 104, (2000), 1686-1694.

42. H. Wei, H. Gu, J. Guo, S. Wei, and Z. Guo, Electropolymerized Polyaniline Nanocomposites from Multi-Walled Carbon Nanotubes with Tuned Surface Functionalities for Electrochemical Energy Storage, Journal of The Electrochemical Society, 160, (2013), G3038-G3045.

43. J. Zhang, J. Tu, D. Zhang, Y. Qiao, X. Xia, X. Wang and C.J. Gu, Multicolor electrochromic polyaniline–WO_3 hybrid thin films: One-pot molecular assembling synthesis, Journal of Materials Chemistry, 21, (2011), 17316-17324.

44. Allen J. Bard, Larry R. Faulkner, Electrochemical Methods Fundamentals and Applications, John Wiley & Sons, Inc. (2001).

45. D.P. Dubal, A.D. Jagadale, S.V. Patil, C.D. Lokhande, Simple route for the synthesis of supercapacitive Co–Ni mixed hydroxide thin films, Materials Research Bulletin 47, (2012), 1239–1245.

46. C.J. Jafta, F. Nkosi, L. le Roux, M.K. Mathe. M. Kebede, K. Makgopa, Y. Song, D. Tong, M. Oyamae, N. Manyala, S. Chen, K.I. Ozoemena, Manganese oxide/graphene oxide composites for high-energy aqueous asymmetric electrochemical capacitors, Electrochimica Acta, (2013), In press, http://dx.doi.org/10.1016/j.electacta.2013.06.096.

47. A.T. Chidembo, K.I. Ozoemena, B.O. Agboola, V. Gupta, G. G. Wildgoose, R.G. Compton, Nickel(II) tetra-aminophthalocyanine modified MWCNTs as potential nanocomposite materials for the development of supercapacitors, Energy Environ. Sci. 3 (2010) 228–236.

List of Figures

Figure 1: SEM images of (a) WO_3 (b) WO_3/PANI

Figure 2: AFM images of (a) WO_3, (b) WO_3/PANI, (c) WO_3 after 1000^{th} charge-discharge cycle, and (d) WO_3/PANI after 1000^{th} charge-discharge cycle.

Figure 3: The absorbance spectrum of the films.

Figure 4: (a) CV curves for the films at 50mVs^{-1}, (b) the CV at 50 and 100 mVs^{-1} for the composite film.

Figure 5: Color change of the composite film during cyclic voltammetry.

Figure 6: (a) Comparative charge–discharge curves of the films measured in 0.5M H_2SO_4 at 0.02mAcm^{-2}, and (b) charge-discharge curves of the films at different current densities.

Figure 7: Comparative cycle stability of the films at 0.16 mAcm^{-2}.

Figure 8: Nyquist plots of the various films at 0.1 V vs Ag/AgCl (sat'd KCl).

Figure 9: Bode plots for the (a) PANI and (b) WO_3/PANI film.

251658240

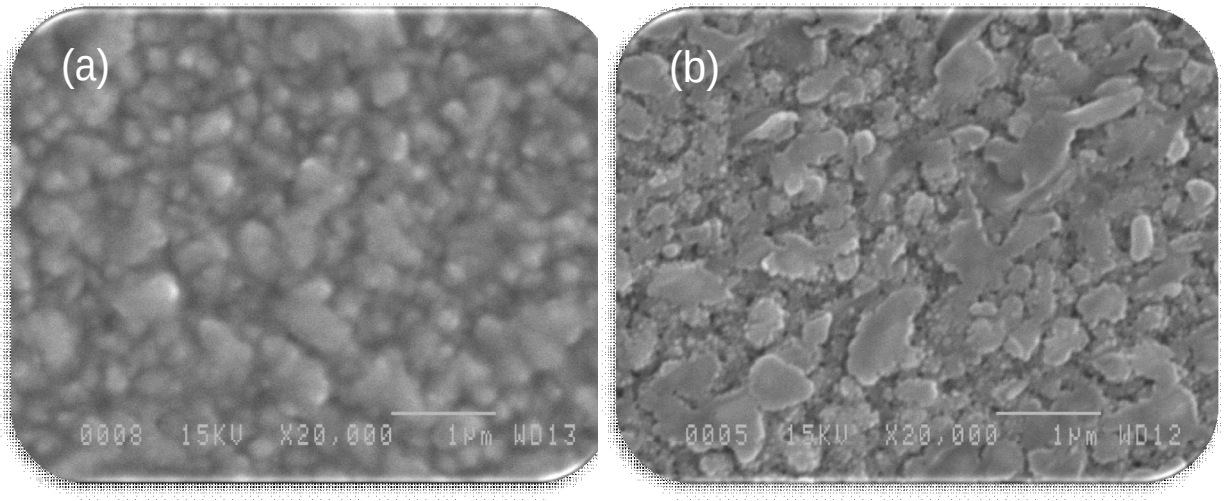

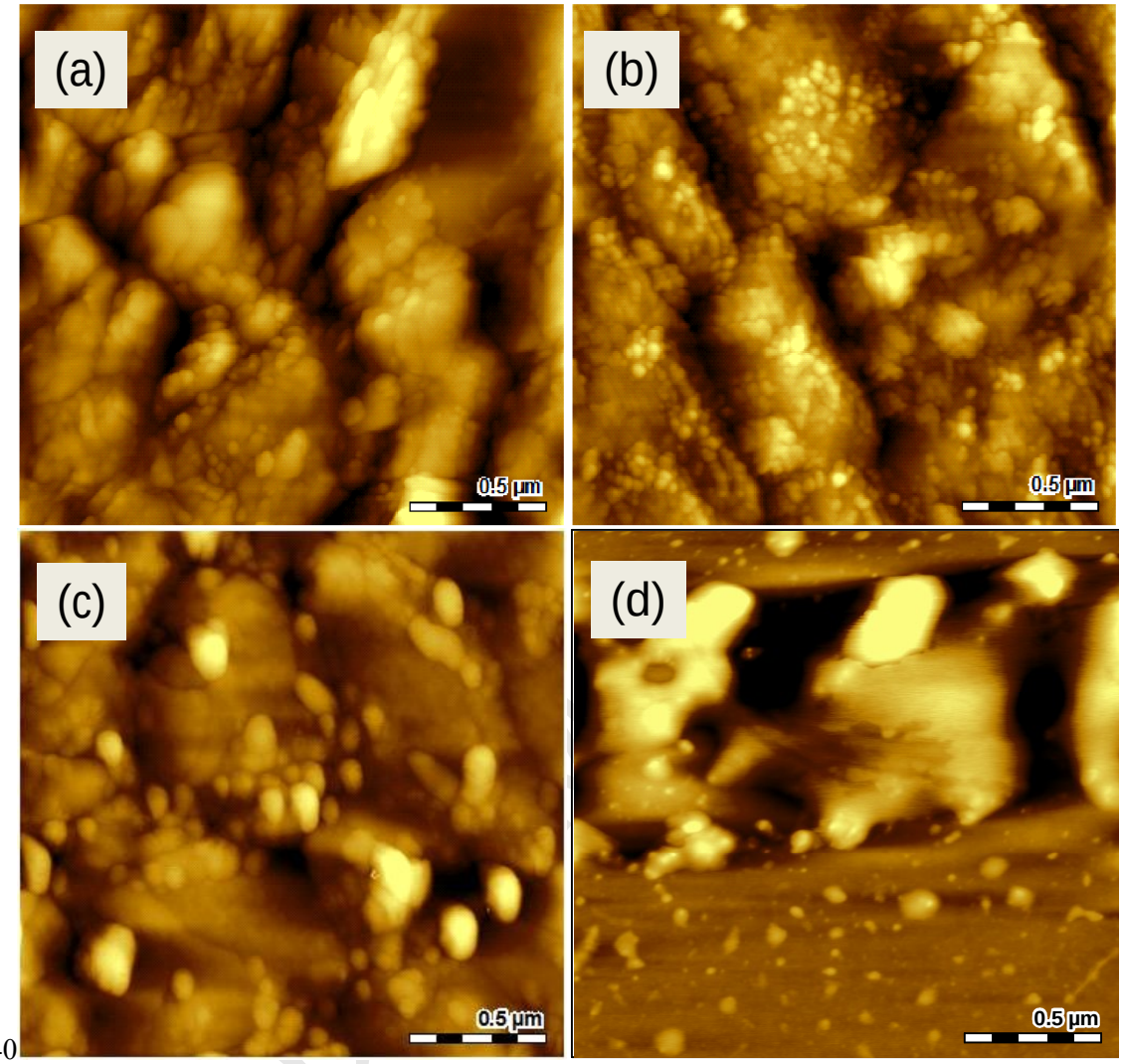

251658240

Figure 2

251658240

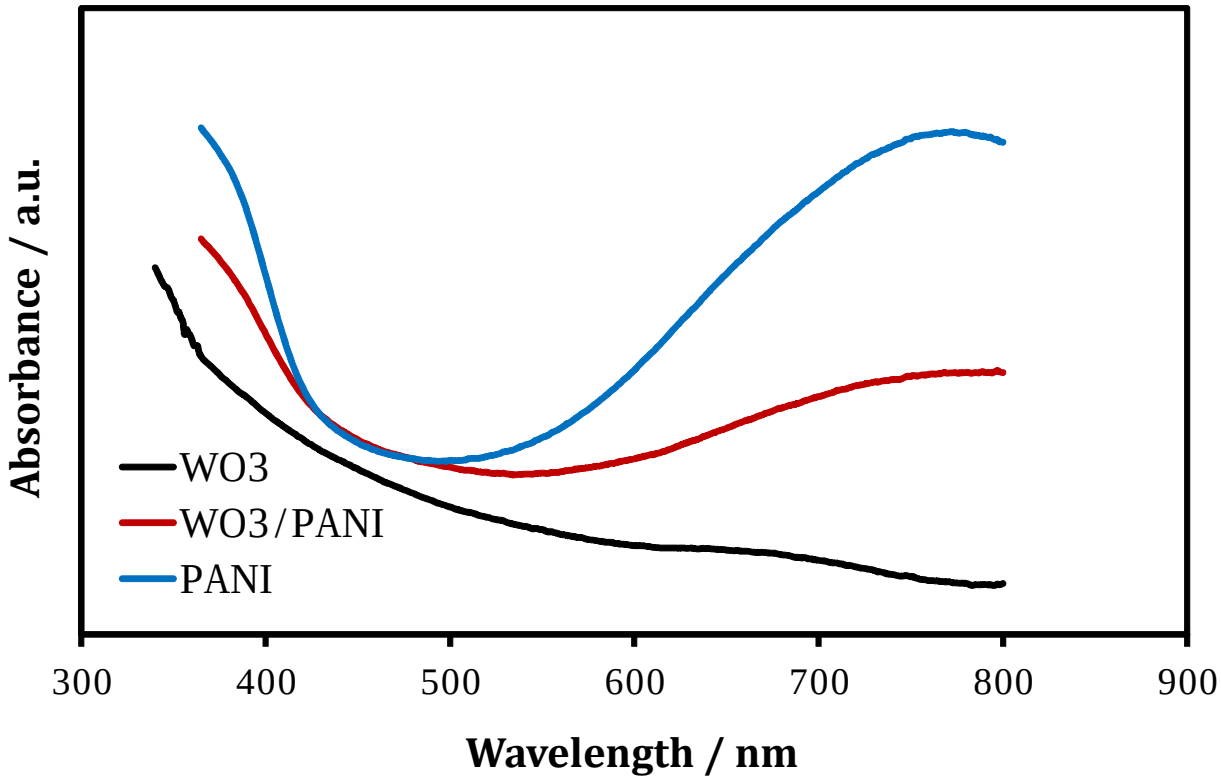

Figure 3

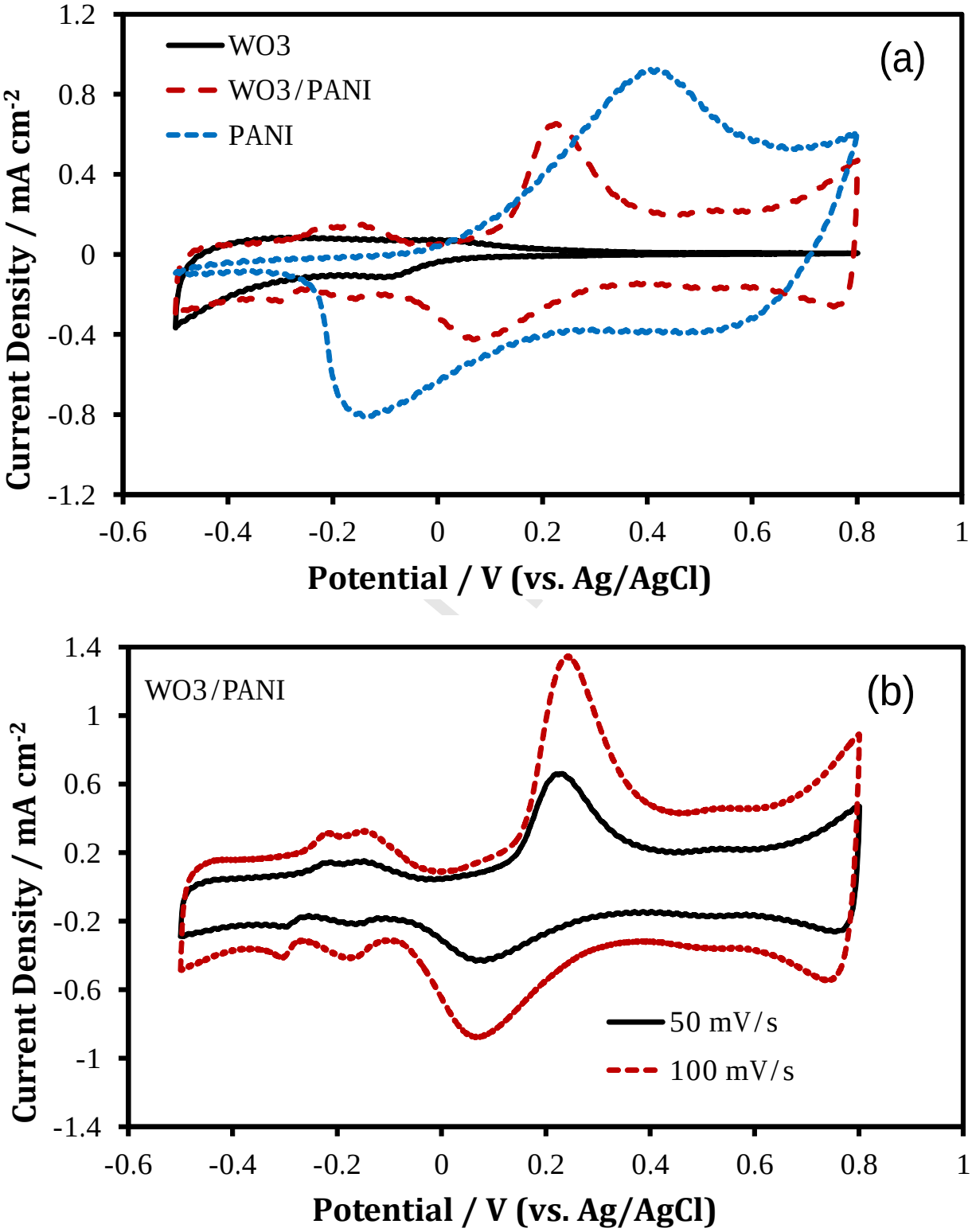

Figure 4

251658240

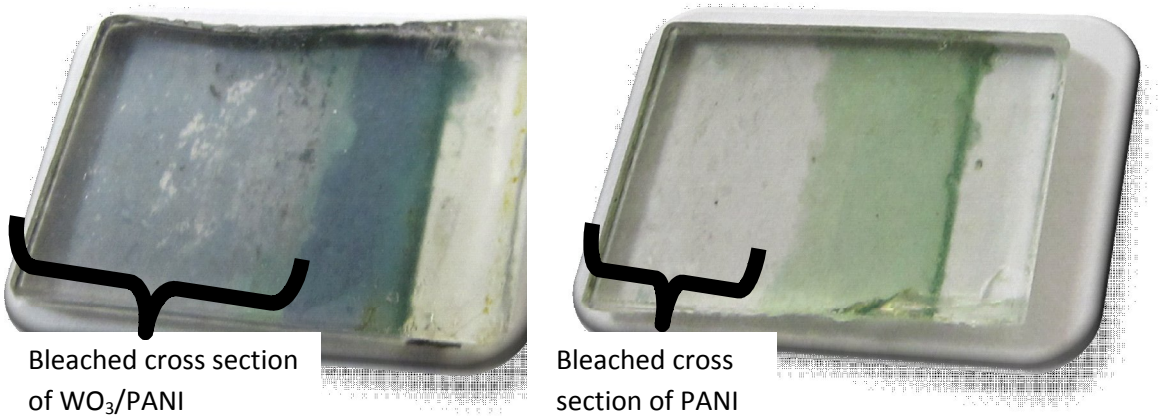

Figure 5

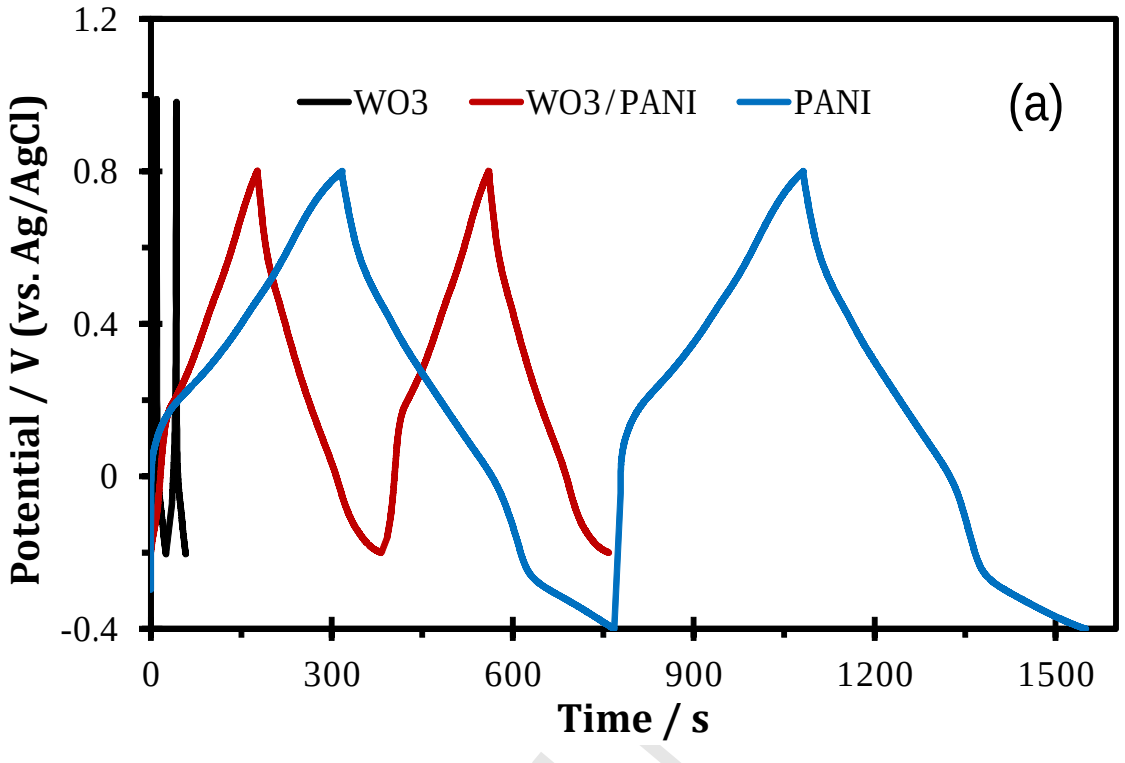

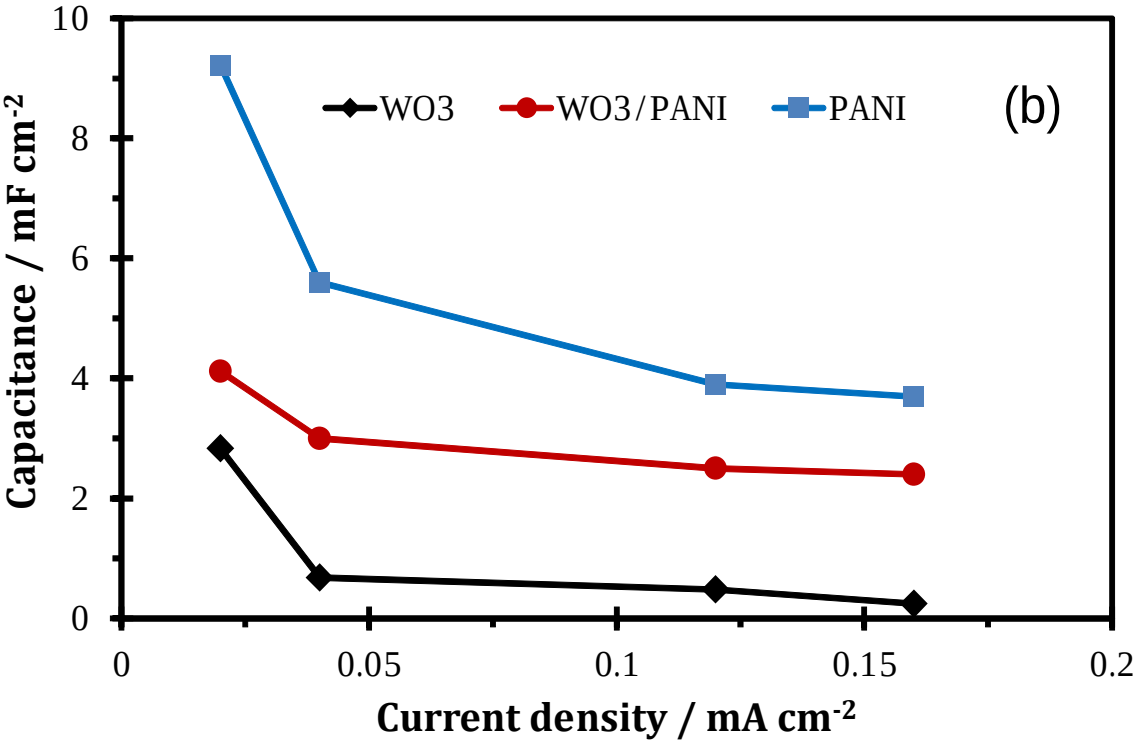

Figure 6

251658240

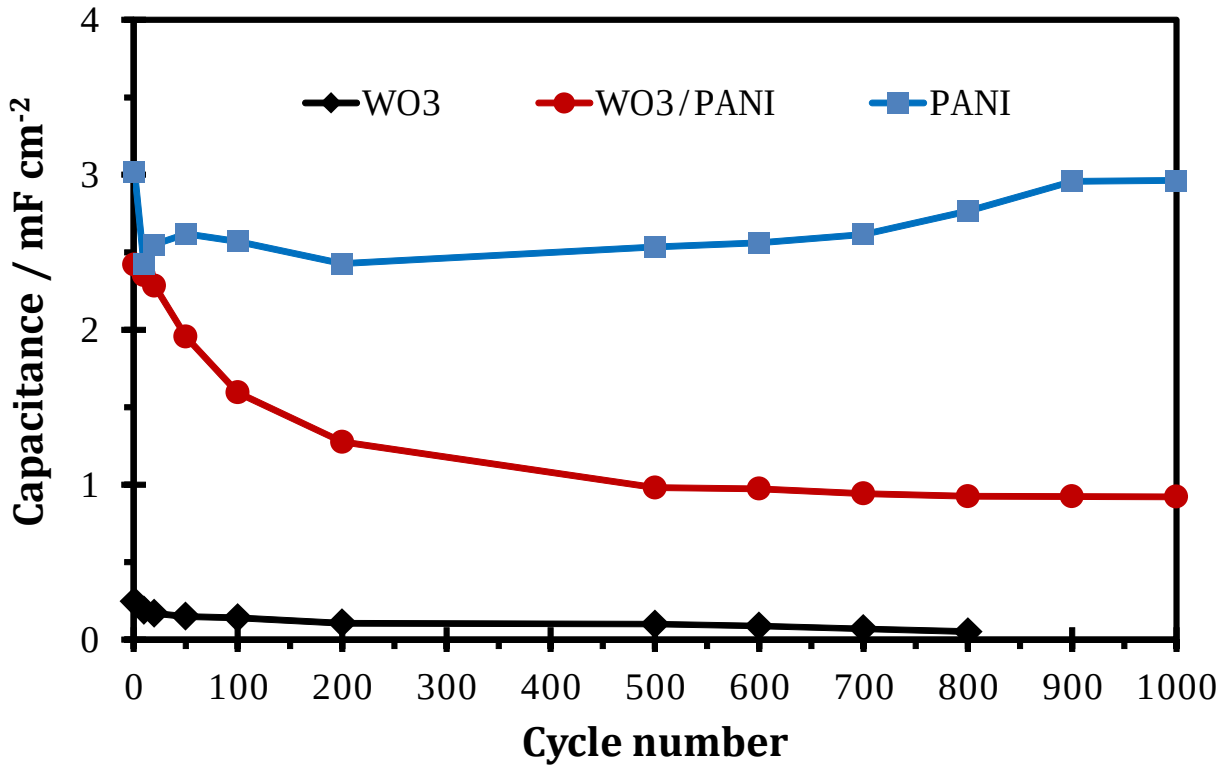

Figure 7

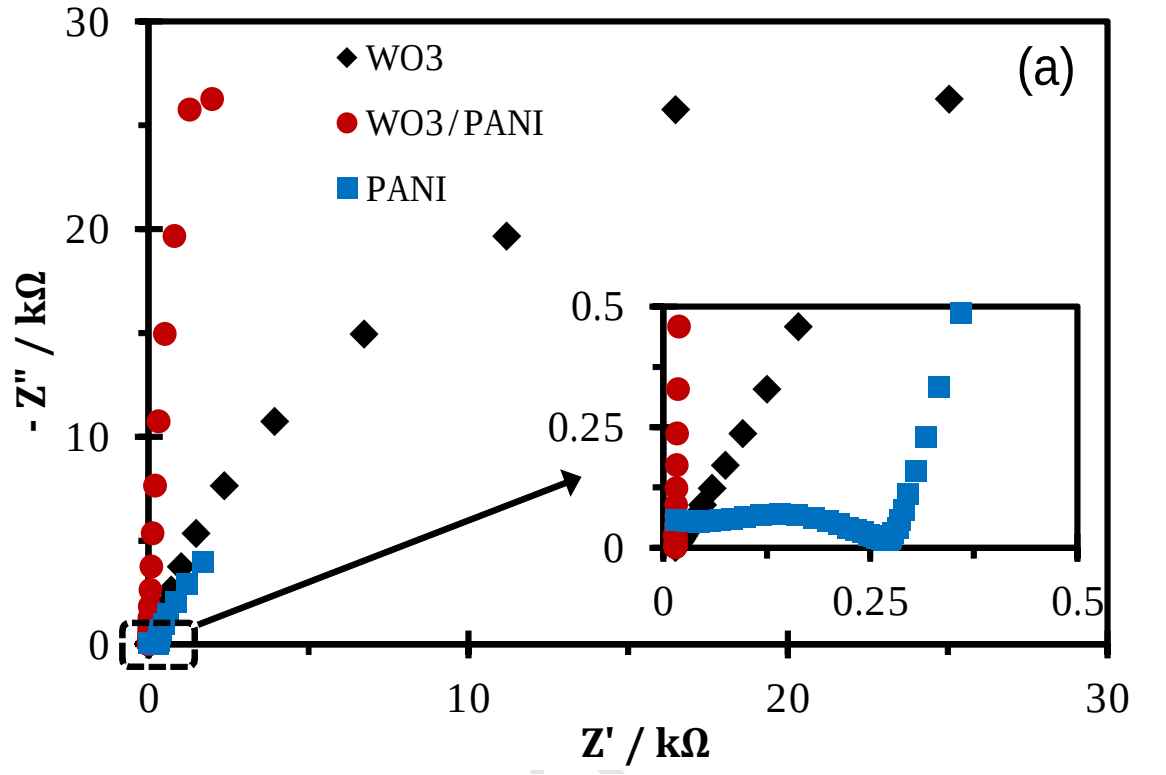

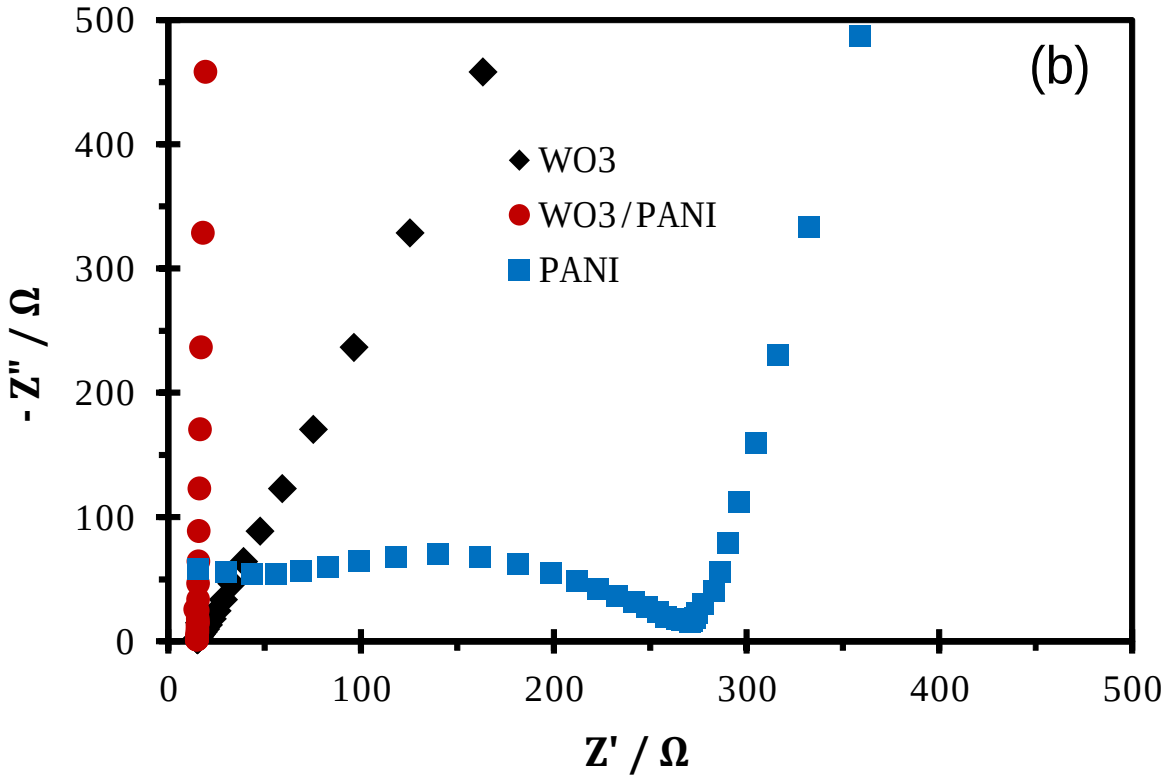

31